Overview of Photoacoustic Imaging in the Medical Diagnostics Field

Viktor Ventsislavov Stoev

Abstract – **The acoustic and optical domains bind in the relatively novel field of photoacoustic imaging, where a short pulse of electromagnetic energy generates an acoustic wave. Capable of delivering high contrast images, the technique is drawing considerable attention as a tool for diagnosis of cancer, lipid deposits, hemoglobin concentration, brain related diseases and many more. The theory of image reconstruction has undergone extensive research in the past 20 years which, coupled with the innovations in signal generation and detection, has successfully advanced the field to the preclinical stage. In this paper we give an overview of the specifics of photoacoustic imaging and elaborate on image reconstruction, signal generation and acquisition.**

Keywords – **Photoacoustic imaging, inversion, laser, transducer**

I. Introduction

Since the discovery of X-rays, medical imaging has played an increasingly important role in the correct diagnosis and treatment of various diseases. This has prompted research institutions, universities and companies to continuously enhance our capabilities of acquiring accurate reconstructions of the inner human body. By now, many imaging techniques have emerged and evolved among which are magnetic resonance imaging (MRI), X-ray computed tomography (CT), ultrasound (US), positron emission tomography (PET), optical coherence tomography (OCT) and others.

In recent years, this pleiad has been enriched by the novel technique of photoacoustic imaging (PAI, also known as optoacoutsic imaging – OAI), which has by now matured to the preclinical stage and will soon become an essential tool for the diagnosis of diseases.

In photoacoustic imaging, acoustic waves are generated by irradiating an optically absorbing media with short pulses of electromagnetic energy. As the energy deposits, a local rise of the temperature occurs. This drives the heated medium to expand rapidly, which is followed by the generation of a mechanical stress in the form of an acoustic wave. This is referred to as the thermo-optical mechanism of stress generation [1]. A typical PA image, recorded with a hydrophone is depicted in Figure 1. Notice the distinct bipolar shape, corresponding to the expansion and shrinking of the heated domain.

The optically absorbing molecules in the human body are called chromophores and their concentration will determine the acoustic wave amplitude. However, the process of signal generation is non-linear, it depends on the concentration of chromophores, but on the laser energy and thermodynamic properties of the tissue as well. Hence, what we observe as an acoustic wave is not directly proportional to the light absorbing molecules concentration, as was initially considered [2]. Nevertheless, light absorption is dominating, which allows for high tissue differentiation - a major difference to ultrasound imaging.

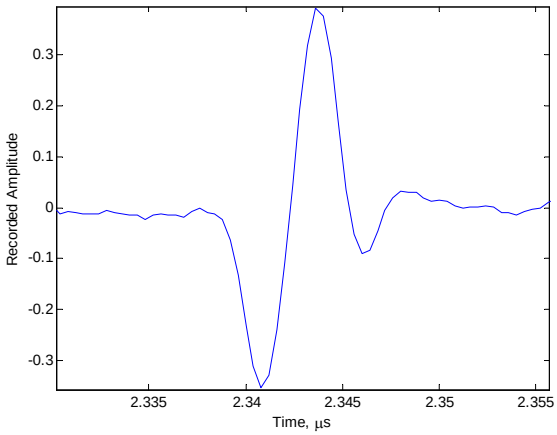

Fig. 1. Acquired photoacosutic signal representing the response of a string of hair to pulsed electromagnetic energy (the signal shape is inverted).

Apart from chromophores concentration, the signal amplitude depends strongly on the irradiation time. If it is sufficiently smaller than the time it takes for the pressure wave to propagate through the illuminated medium, the amplitude will be maximum. This is known as the stress confinement rule [3] and is the reason why nanosecond excitation sources are used in PAI.

Another distinguishing feature between ultrasound imaging and PAI is that the latter depends not only on the acoustic properties of the irradiated volume, but on the optical ones as well. The optical domain characteristics determine the penetration depth (it is deemed as the depth at which light becomes diffuse), as well as the signal amplitude, since absorption is wavelength dependent. Typically, wavelengths in the 600-900nm range are used, as penetration there can extend to several centimeters, but other wavelengths as short as 400nm and as long as 1210nm are also utilized [4]. Once the illuminated region relaxes and the acoustic wave starts to propagate, the acoustic domain properties take place into shaping the signal. The signal undergoes acoustic attenuation(A), diffraction(D), acoustic wave reflection and transmission(T). Their effect is cumulative and we denote it here asψ, where

$$\psi = TDA \tag{1}$$

These parameters define the profile of the photoacoustic signal, the bandwidth and the amplitude. A typical

V. Stoev is with the Department of Electronics and Electronics Technologies, Faculty of Electronic Engineering and Technologies, Technical University - Sofia, 8 Kliment Ohridski blvd., 1000 Sofia, Bulgaria, e-mail: v.stoev@tu-sofia.bg

bandwidth in the tissue will span the 1 – 30 MHz range, with the amplitude of the acoustic pressure not exceeding 10kPa and the penetration depth extending to a few centimeters at best. However, these characteristics allow for a remarkably broad area of applications.

Photoacoustic imaging is suitable for blood vessel imaging and differentiation between oxygenated and deoxygenated blood, as blood is a very strong light absorber in the near-infrared region [5]. Since tumours exhibit a high microvessel density (angiogenesis in medical terms), this malignant area will show an increased level of absorption of laser light which, coupled with the high spatial resolution of PAI can be used for the detection of breast cancer [6]. Other biomedical applications include imaging of lipid deposits found in atherosclerotic plaques with wavelength of 1210nm, intravascular imaging, photoacoustic microscopy, imaging of the brain vasculature, joints and combined US-PA imaging.

In this paper, we overview different approaches to image reconstruction and photoacoustic signal generation. We focus on the model-based reconstruction method and provide several experimental results that highlight some of the applications and problems intrinsic to the photoacoustic imaging technique.

II. Theoretical Backgrounds

Imagine a volume filled with liquid with isotropic characteristics and a laser light source, capable of delivering short impulses of EM energy that meet the stress and thermal confinement requirements (heat must not dissipate during the heating process). Then a photoacoustic signal will be generated which, in the linear approximation, can be described as [7]

$$\nabla^2 p(\mathbf{x},t) - \frac{1}{c^2}\frac{\partial^2}{\partial t^2}p(\mathbf{x},t) = -\frac{\beta}{C_p}\frac{\partial H(\mathbf{x},t)}{\partial t} \qquad (2)$$

Formula (2) is known as the photoacoustic wave equation, where$p$ is the acoustic wave pressure (in Pa) and c is the speed of propagation. The source term (the right-hand side) contains two parameters namely, the specific heat capacity C_p, and the volume thermal expansion β. The source denoted as $H(\mathbf{x},t)$, is the so-called heating function and it shows us the heat deposited in the illuminated object per unit volume per unit time. The function is explicitly given as $H(\mathbf{x},t) = \mu_a(\mathbf{x})F(\mathbf{x},t)$, where the second term represents the laser fluence rate at a point in the object while, $\mu_a(\mathbf{x})$ is the absorption of the structure. It should be noted that the fluence rate depends not just on the laser source characteristics, but on the absorption (and scattering) of the structure as well. This gives a nonlinear relationship between the generated signal and the absorption occurring in the illuminated object. This is why we say that the photoacoustic images are absorption dominated, but not linearly proportional to the absorption.

A solution to equation (2) for the pressure p is the starting point for image reconstruction. Following a Fourier domain procedure a forward solution to the problem can be found by first applying a Laplace transform over the temporal component and a 3-D Fourier transform over the spatial component. The result is the $(\mathbf{k}, s)$ domain expression for the PA wave equation, which written in terms of the spectral domain Green's function is given as

$$\tilde{p}(\mathbf{k},s) = \frac{\Gamma}{c^2}\tilde{G}(\mathbf{k},\mathrm{s})s\tilde{H}(\mathbf{k},s) \qquad (3)$$

Where $\tilde{G}(\mathbf{k},\mathrm{s}) = \frac{1}{(\mathbf{k}^2+\gamma^2)}$ is the Green's function, $\gamma^2 = \frac{s^2}{c^2}$, $\mathbf{k}^2 = (\mathrm{k}\cdot\mathrm{k})$ and $\Gamma = \frac{c^2\beta}{C_p}$. The latter coefficient is called the Grüneisen coefficient, it is dimensionless and equals approximately 0.11 for water at room temperature.

However, a solution in the time domain or in frequency domain is more intuitive. Applying the inverse 3D Fourier transform to equation (3) we arrive at the desired solution in frequency domain expressed as

$$\hat{p}(\mathbf{x},s) = \frac{\Gamma}{c^2}s\int\limits_{\mathbf{x}'\in\mathbb{D}_H}\hat{\mathrm{G}}(\mathbf{x}-\mathbf{x}',\mathrm{s})\hat{H}(\mathbf{x}',s)\mathrm{d}V \qquad (4)$$

where $\mathbb{D}_H$, is the illuminated volume. To find an explicit solution to this problem in frequency domain, the inverse Fourier transform of the spectral domain Green's function is needed. For this purpose we introduce spherical coordinates, carry out the integration and use residual calculus for the integration over the radial distance [8]. The result from these steps is the solution to the photoacoustic wave equation in $(\mathbf{x},\mathrm{s})$ domain, given as

$$\hat{p}(\mathbf{x},s) = \frac{\Gamma}{c^2}s\int\limits_{\mathbf{x}'\in\mathbb{D}_H}\frac{\mathrm{e}^{-\gamma|\mathbf{x}-\mathbf{x}'|}}{4\pi\mid\mathbf{x}-\mathbf{x}'\mid}\hat{H}(\mathbf{x}',s)\mathrm{d}V \qquad (5)$$

Two approaches can be followed from here. Move to the frequency domain by taking $s = \mathrm{j}\omega$, or move to time domain by taking the inverse Laplace transform. If we consider the latter case, the solution to the wave equation based on the Green's function for lossless, homogeneous background is given in [9] as

$$p(\mathbf{x},t) = \frac{\beta}{4\pi C_p}\iiint\frac{\mathrm{d}\mathbf{x}'}{\mid\mathbf{x}-\mathbf{x}'\mid}\frac{\partial H(\mathbf{x}',t')}{\partial t'}\bigg|_{t'=t-\frac{|\mathbf{x}-\mathbf{x}'|}{c}} \qquad (6)$$

where x and x' denote the positions of the receiver and source respectively.

An important assumption, which is valid for soft tissue, is that the light pulse is short enough for thermal diffusion not to occur. This is referred to as thermal confinement. With this assumption, the delivered energy can be modeled as the product of a Dirac delta pulse and a spatially varying heating function. Then equation (6) is rewritten into a more explicit form, highlighting the received signal dependence on the initial pressure distribution p_0, as

$$p(\mathbf{x},t) = \frac{\partial}{\partial t}\left[\frac{t}{4\pi}\iint_{|\mathbf{x}-\mathbf{x}'|=ct}p_0(\mathbf{x}')\mathrm{d}\Omega\right] \qquad (7)$$

The key to image reconstruction is finding the initial pressure distribution from data recorded at different locations, outside the imaged volume, which is nothing else but the inversion of equation (7). This starting point to

image reconstruction has been used by Kruger *et al.* for filtered back-projection algorithms based on the Radon transform described in [10]. Xu *et al.* tested another algorithm, based on the Radon transform approximation with a Hilbert transform [11]. Other time-domain solutions include deconvolution algorithms [12] as well as back-projection and synthetic aperture algorithms borrowed from the ultrasound field. A model-based reconstruction approach was developed by Razansky *et al*. showing the advantages of numerical solutions [13].

Other researchers concentrated on the frequency domain algorithms. For example, Xu and Wang [14,15], developed exact frequency domain reconstruction algorithms for spherical, cylindrical and planar geometry. A more recent paper suggests that constructing an algorithm which includes the boundary conditions at the tissue-air interface might be a better choice, since this boundary is significantly affecting the received pressure. The suggested method uses a back-propagation algorithm to estimate the absorbers [16]. Cox *et al.* have proposed a fast method for calculating PA fields in liquids by applying wavenumber integral techniques from the seismic world [17].

If $s = \mathrm{j}\omega$ is substituted in Eq. (7) the explicit solution to the forward problem in frequency domain, discretized (using the mid-point rule) and rewritten as a data model for several receiver locations is given as

$$\hat{\mathbf{p}} = \hat{\mathbf{G}}\hat{\mathbf{H}} \tag{8}$$

where $\hat{\mathbf{p}}$ represents the received pressure in frequency domain for a linear array transducer, $\hat{\mathbf{G}}$ is the Green's function matrix and $\hat{\mathbf{H}}$ is a vector representing the sources.

Inverting this equation by applying the adjoint operator gives

$$\hat{\mathbf{H}} = \hat{\mathbf{G}}^{\mathrm{H}}\hat{\mathbf{p}} \tag{9}$$

where $\hat{\mathbf{G}}^{\mathrm{H}}$ is the hermitian transpose of the Green's matrix.

Equation (9) is a basic imaging procedure which is a computationally simple and stable tool for reconstructing images as it includes no matrix inverses. Although not as sophisticated as other PAI techniques, it can deliver accurate images with good quality which can be exploited in more complex algorithms. An example in-vivo image, showing a B-scan of a human forehand and underlying vasculature, reconstructed with the above imaging procedure can be observed in Figure 2. Notice that the strongest light absorbers are the skin and the blood vessels which contain the largest concentration of chromophores absorbing at 650nm.

III. METHODS

A. Instrumentation

The effective generation and registration of photoacoustic signals has also undergone extensive research, evolving in parallel to the image reconstruction.

The generation of photoacoustic signals is primarily achieved by two types of sources – powerful laser diodes capable of delivering short pulses (~100ns) with high pulse repetition rate (PRF) gravitating around 1kHz, and tunable NIR ND:YAG lasers with low PRF between 10-20Hz, but with very high energy output and very short pulse length (~30 mJ and ~10 ns respectively) [18].

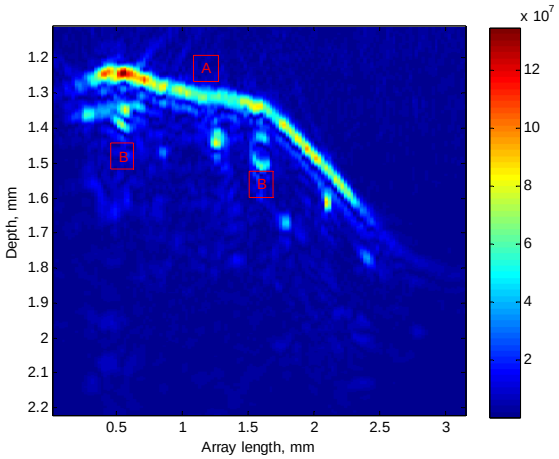

Fig. 2. Image of the skin surface and underlying blood vessels. The continuous strong signal is the skin (A), while the smaller round images are blood vessels (B).

Other laser system are also utilized, some custom build (using arrays of laser diodes at two different wavelengths) while some are commercially available and can deliver pulses with 6ns duration. In either of these cases, the goal is to achieve the conditions of stress confinement and thermal confinement.

Recently, multi-wavelength PAI systems are gaining considerable attention. Tunable NIR lasers have high power output, but are bulky and often require cooling. In comparison, laser diodes are small and do not require cooling, while achieving high PRF. This allows for signal averaging and is the reason why several laser diodes at different wavelengths are fused together with custom build transducers and used as a dual-imaging solution – PAI and ultrasound [19].

The generated photoacoustic signals tend to be very broadband spanning the 1-100MHz range. However, tissue is acting as a low-pass filter, limiting this range to several MHz, usually up to 10(30)MHz. This is still a very broad frequency band which is only partially covered by commercially available ultrasonic transducers (which are usually employed for PAI). They typically have a central frequency at several MHz and a high Q-factor.

However, as the field is maturing, array transducers specifically designed for PAI are emerging. For example, the Vevo 2100, VisualSonics, photoacoustic system is equipped with a linear array transducer (MS250) with fc= 21 MHz, consisting of 256 elements. Another example is the 30MHz piezo-composite linear array, which is a part of a custom build multi-channel receiver system [20].

B. Acquisition system

A typical acquisition system for photoacoustic imaging resembles any ultrasound system with the exception of the source – in photoacoustics it is a powerful EM wave emitter.

Several commercially available PAI systems have emerged in recent years. Some of these are the abovementioned Vevo 2100 from VisualSonics, another one is the Nexus 128 Preclinical Photoaocustic CT Scanner from Endra Life Sciences and the MSOT inSight / inVision by iThera Medical. As the field is rapidly expanding, more will definitely follow in the near future.

IV. Discussion and Conclusion

Although a rapidly developing field, photoacoustic imaging is still a relatively new technique which faces many problems from both technological and signal processing perspective.

Among all the challenges (and a major drawback) is the low signal-to-noise-ratio (SNR), intrinsic to the photoacoustic field. Apart from limiting the reconstruction accuracy (respectively diagnosis accuracy) it is also the major problem when we consider imaging depth. The most intuitive and easily achievable improvement here is averaging, which if applied over a sufficient number of acquisitions will mitigate noise and increase the SNR. This is why laser diodes are particularly attractive for PAI, as averaging over a few hundred samples can be easily achieved. Other methods for SNR improvement include averaging and normalization (L2 and L1 norm), different signal processing techniques (borrowed directly or modified respectively from other fields), as well as application of contrast agents for improved absorption [21].

From technological point of view, the major challenges include the design of broadband transducers and their integration with the light delivery system. Companies and international projects have successfully developed several such integrations with more following in the near future. An example is the MSOT system by iThera Medical [22] or the FULLPHASE project [19].

Acknowledgements

The author would like to thank Assoc Prof M. Mitev and Prof I. Iliev for their invaluable input.

This work is supported under project grant N:152ПД0049-03 by the Technical University of Sofia.

References

[1] C. G. A. Hoelen and F. F. M. de Mul. *A new theoretical approach to photoacoustic signal generation.* Acoustical Society of America Journal, 106:695–706, August 1999

[2] Paul Beard. *Biomedical photoacoustic imaging. Interface Focus*, 1(4):602–631, 2011.

[3] Alexander A. Oraevsky, Steven L. Jacques, and Frank K. Tittel. *Measurement of tissue optical properties by time-resolved detection of laser-induced transient stress*. Appl. Opt., 36(1):402–415, Jan 1997.

[4] Minghua Xu and Lihong V. Wang. *Photoacoustic imaging in biomedicine*. Review of Scientific Instruments, 77(4):041101+, 2006.

[5] X. Wang, X. Xie, G. Ku, L. V. Wang, and G. Stoica, "*Noninvasive imaging of hemoglobin concentration and oxygenation in the rat brain using high-resolution photoacoustic tomography*," J Biomed Optic, vol. 11, no. 2, pp. 024 015/1 – 024 015/9, 2006.

[6] Robert A. Kruger, Richard B. Lam, Daniel R. Reinecke, Stephen P. Del Rio, and Ryan P. Doyle. *Photoacoustic angiography of the breast*. Medical Physics, 37(11):6096–6100, 2010.

[7] V. E. Gusev and A. A. Karabutov, *Laser Optoacoustics*, AIP, New York, 1993.

[8] J.T. Fokkema, P.M. van den Berg. "*Seismic applications of acoustic reciprocity*". Elsevier, 1993.

[9] Minghua Xu and L.V. Wang. *Time-domain reconstruction for thermoacoustic tomography in a spherical geometry*. Medical Imaging, IEEE Transactions on, 21(7):814–822, 2002.

[10] Robert A. Kruger, Daniel R. Reinecke, and Gabe A. Kruger. Thermoacoustic computed tomography–technical considerations. Medical Physics, 26(9):1832–1837, 1999.

[11] Y. Xu, L.-H. Wang, G. Ambartsoumian, and P. Kuchment, Med. Phys.31,724, 2004.

[12] Yi Wang, Da Xing, Yaguang Zeng, and Qun Chen. *Photoacoustic imaging with deconvolution algorithm*. Physics in Medicine and Biology, 49(14):3117, 2004.

[13] Dean-Ben, X.L.; Buehler, A.; Ntziachristos, V.; Razansky, D., "*Accurate Model-Based Reconstruction Algorithm for Three-Dimensional Optoacoustic Tomography*," Medical Imaging, IEEE Transactions on , vol.31, no.10, pp.1922,1928, Oct. 2012 doi: 10.1109/TMI.2012.2208471

[14] Yuan Xu, Dazi Feng, and L.V. Wang. *Exact frequency-domain reconstruction for thermoacoustic tomography. i. planar geometry*. Medical Imaging, IEEE Transactions on, 21(7):823–828, 2002.

[15] Yuan Xu, Minghua Xu, and L.V. Wang. *Exact frequency-domain reconstruction for thermoacoustic tomography. ii. cylindrical geometry*. Medical Imaging, IEEE Transactions on, 21(7):829–833, 2002.

[16] Habib Ammari, Emmanuel Bossy, Vincent Jugnon, and Hyeonbae Kang. *Mathematical modeling in photoacoustic imaging of small absorbers*. SIAM Rev., 52(4):677–695, November 2010.

[17] B. T. Cox and P. C. Beard. *Fast calculation of pulsed photoacoustic fields in fluids using k-space methods*. The Journal of the Acoustical Society of America, 117(6):3616–3627, 2005

[18] T J Allen and P C Beard. *Dual wavelength laser diode excitation source for 2D photoacoustic imaging*. In Biomedical Optics (BiOS) 2007, pages 64371U–64371U. International Society for Optics and Photonics, 2007.

[19] http://cordis.europa.eu/project/rcn/104914_en.html

[20] Bitton, R.; Zemp, R.; Yen, J.; Wang, L.H.; Shung, K.K., "*Design of a High Frequency Array Based Photoacoustic Microscopy System for Micro-Vascular Imaging*," Engineering in Medicine and Biology Society, 2007. EMBS 2007. 29th Annual International Conference of the IEEE , vol., no., pp.2175,2178, 22-26 Aug. 2007

[21] Ku, G. & Wang, L. V. 2005 *Deeply penetrating photoacoustic tomography in biological tissues enhanced with an optical contrast agent*. Opt. Lett.30, 507 –509.

[22] Andreas Buehler, Marcin Kacprowicz, Adrian Taruttis, and Vasilis Ntziachristos, "*Real-time handheld multispectral optoacoustic imaging*," Opt. Lett. 38, 1404-1406 (2013)